REPORT DOCUMENTATION PAGE	Form Approved OMB NO. 0704-0188

1. AGENCY USE ONLY (Leave Blank)	2. REPORT DATE	3. REPORT TYPE AND DATES COVERED Final Report 2/1/06 - 6/30/06

4. TITLE AND SUBTITLE ERC SimCenter U2NCLE Unstructured Flow Solver for Rotorcraft M&S HI-ARMS Technical Objective A-TC-3	5. FUNDING NUMBERS W911NF-06-1-0048
6. AUTHOR(S) Chunhua Sheng, David Marcum, Xiao Wang and Kevin Sutherland	
7. PERFORMING ORGANIZATION NAME(S) AND ADDRESS(ES) ERC SimCenter Mississippi State University P. O. Box 9627 Mississippi State, MS 39762	8. PERFORMING ORGANIZATION REPORT NUMBER MSSU-COE-ERC-05-06
9. SPONSORING / MONITORING AGENCY NAME(S) AND ADDRESS(ES) U. S. Army Research Office P.O. Box 12211 Research Triangle Park, NC 27709-2211	10. SPONSORING / MONITORING AGENCY REPORT NUMBER 50387.1-EG

11. SUPPLEMENTARY NOTES

The views, opinions and/or findings contained in this report are those of the author(s) and should not be construed as an official Department of the Army position, policy or decision, unless so designated by other documentation.

12 a. DISTRIBUTION / AVAILABILITY STATEMENT	12 b. DISTRIBUTION CODE
Approved for public release; distribution unlimited.	

13. ABSTRACT (Maximum 200 words)

The objective of this study is to conduct unstructured solver performance evaluation for HPC Institute for Advanced Rotorcraft Modeling and Simulation (Hi-ARMS). The Mississippi State University unstructured flow solver U2NCLE is evaluated based on a common test problem, NACA0015 wing. Computational results on Cp, lift, and drag coefficients of the wing are presented using preconditioned and non-preconditioned schemes. Computational statistics on CPU time, memory requirements, and parallel efficiency of the solver are collected based on a Linux cluster using 32, 64,128 and 256 processors. In addition, optional deliverables are provided for solutions on a realistic helicopter rotor undergoing high-frequency blade-pitch oscillation. Computational capabilities are demonstrated for simulating the unsteady flowfield associated with complex rotor blade motion, which are useful for investigating rotor/wake/fuselage interactional aerodynamics.

14. SUBJECT TERMS Rotorcraft, Unstructured Grid, NACA 0015 Wing	15. NUMBER OF PAGES 23 pages for final report submitted electronically
	16. PRICE CODE

17. SECURITY CLASSIFICATION OR REPORT	18. SECURITY CLASSIFICATION ON THIS PAGE	19. SECURITY CLASSIFICATION OF ABSTRACT	20. LIMITATION OF ABSTRACT
UNCLASSIFIED	**UNCLASSIFIED**	**UNCLASSIFIED**	**UL**

NSN 7540-01-280-5500

Standard Form 298 (Rev.2-89)
Prescribed by ANSI Std. 239-18
298-102

Enclosure 1

HI-ARMS Technical Objective A-TC-3: Unstructured Solver Performance Evaluation

Final Report (Grant W911NF-06-1-0048)

Prepared for

Dr. Robert Meakin
U.S. Army Aeroflighydynamics Directorate
NASA Ames Research Center
Moffett Field, CA 94035

By

Chunhua Sheng, David Marcum, Xiao Wang, and Kevin Sutherland

Report MSSU-COE-ERC-05-06

Computational Simulation and Design Center
May 2006

Mississippi State University
P.O. Box 9627
Mississippi State, MS 39762

1. Objectives

The objective of the current grant is to conduct Unstructured Solver Performance Evaluation activity for HPC Institute for Advanced Rotorcraft Modeling and Simulation (HI-ARMS). Specified deliverables are provided to the HI-ARMS evaluation team for solutions and computational statistics for a common test problem on a NACA0015 wing, and optional deliverables are provided for solutions on a realistic helicopter rotor, which will be used as the basis for measuring the attributes of the current unstructured solver to meet long-term HI-ARMS objectives and program requirements.

2. Computational Approach

The tasks under the current grant have been conducted with an unstructured flow solver referred to as U^2NCLE (**U**nstructured **Un**steady **C**omputation of Fie**l**d **E**quations). It is a portable, scalable parallel version of the three-dimensional unsteady Reynolds-averaged Navier-Stokes flow solver developed at the Computational Simulation and Design Center (SimCenter) at Mississippi State University. The essential elements of this capability are 1) a dynamic mixed-element unstructured grid generation procedure, 2) a portable scalable parallel implicit viscous flow solver, 3) a 6-DOF trajectory analysis integrated with the flow solver for maneuvering predictions, and 4) a visualization/animation system capable of processing very large unsteady three-dimensional datasets. The computational simulation methodology used has evolved over eighteen years. Detailed accounts of the unstructured grid generation procedures and flow solvers employed here are given in previous publications [1-9].

The present report will focus on specific topics related to the required deliverables as outlined in the HI-ARMS Invitation to Submit for Proposal for the common test problem, the NACA0015 wing, and computed results obtained during this investigation for the optional test problem, a generic but realistic three-bladed rotor. A summary of capabilities developed and demonstrated for rotorcraft related simulations is given here. A discussion of various computational simulations and statistics obtained for the test problems then follows.

2.1 Multi-Element Unstructured Grid Generation

The SimCenter's unstructured grid generation system (SolidMesh) was used to generate all of the grids used here. SolidMesh first generates surface grids for all surfaces, and then uses the Advancing Front Local Reconnection scheme (AFLR) to generate high-quality volume grids. The unstructured grid generation schemes used here are given in [1-3]. Implicit flow simulation algorithms are used to enable high resolution of viscous sublayer regions near solid boundaries. Tetrahedral elements are not well suited for accuracy in viscous regions. Viscous flow accuracy can be improved by using mixed element types. A multi-element capability has been developed for this purpose and used in the wing and rotor configurations. The mixed element capability utilizes prisms in viscous regions near the solid boundaries and tetrahedral elements in inviscid regions, with pyramidal elements for blending between these regions. Mixed element types also provide a very substantial improvement in efficiency and run time because the number of edges is greatly reduced below that required for tetrahedral elements, and most of the computational labor of solution is contained in loops over edges. Hexahedral elements are also supported but were not used here.

Three unstructured meshes were generated for the NACA0015 wing configuration, which include 1.57, 3.66, and 7.0 million node points, respectively. The first mesh (1.57M) has a coarser surface grid resolution, and points are not packed near the wing tip. The third mesh (7.0M) uses fully unstructured surface representation for the wing surface, and has much more refined trailing edge. The second mesh (3.66M) has a similar surface point distribution as provided by HIARM in the guideline for the common test problem. Therefore, it has been selected for the unstructured solver performance evaluation, see Figure 1. The initial spacing off the wing surface is 1.0×10^{-5}, which results in an average y+ value of 0.62 on the wing surface at the free stream Mach number of 0.1235 and a Reynolds number of 1.5 million.

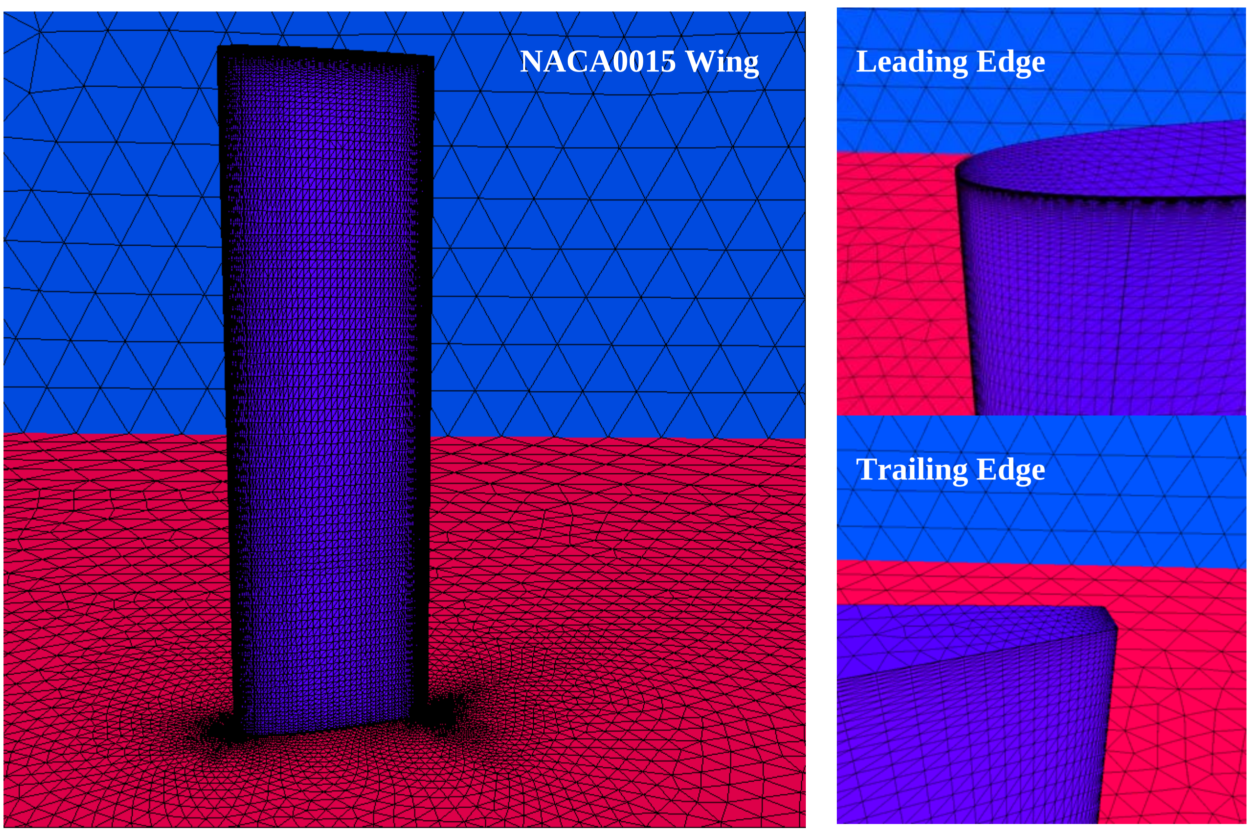

Figure 1 – Surface meshes for the common test problem:
NACA0015 wing with 3.66M node points

2.2 Portable Scalable Parallel Implicit Solution Algorithm

U^2NCLE is a portable, scalable parallel flow solver developed for use with multi-element unstructured grid topologies that provides all the capabilities needed for the present common and optional test problems. The parallel algorithms used here [4-9] have evolved over the past fifteen years from previous sequential algorithms for the unsteady Reynolds-averaged Navier-Stokes equations. The parallel flow solver employs a domain decomposition to define and distribute work among multiple processors, and to utilize distributed memory associated with multiple processors. The solution algorithm uses an iterative implicit algorithm at each time step, applying symmetric Gauss-Seidel relaxation as the innermost iteration, to provide scalable concurrency. Portability across numerous parallel computing platforms is maintained using the MPI message-passing library for interprocessor communications.

There are three versions of the unstructured solver in the U^2NCLE simulation package: an incompressible version that solves artificial compressibility form of governing equations, a compressible solver, and an arbitrary Mach number solver that uses a global preconditioning technique. A thorough discussion of the incompressible flow solver as formulated for steady flow problems is given in [4]. Discussions of the arbitrary Mach number flow solver as formulated for both unstructured and structured grids are given in [8,9]. Simulations for the wing and rotor configurations were conducted with the arbitrary Mach code that is capable of solving both low- and high-speed flows. A simulation and prediction capability for a tiltrotor that includes the actual rotating blades and an icing model have been undertaken to develop a physics-based maneuvering simulation and prediction capability for complete rotorcraft configurations [10]. A unique feature of the U^2NCLE solver is that it provides a physics-based capability to simulate the complex flow behavior and maneuvering characteristics for complete tiltrotor aircraft that includes rotating components, such as the rotating blades undergoing cyclic blade-pitch motion. The complex geometries are addressed using dynamic multi-element unstructured grids with the capability of moving and distorting grid motion to handle moving appendages and rotating blades. The numerical algorithm is developed based on a node-centered finite-volume implicit scheme. Newton subiterations are used to advance the time-step, and symmetric Gauss-Seidel relaxations are used to solve the linear system of equations at each time-step. A first- or second-order temporal accuracy can be used for time-accurate unsteady simulations. An inviscid flux is calculated using a modified (preconditioned) Roe scheme, and 2^{nd}-order spatial accuracy is achieved by using a least-squares reconstruction procedure. Viscous effects are modeled using a Spalart-Allmaras turbulence model, or k-ε, k-ω, and q-ω two-equation turbulence models.

The following notable capabilities of the U^2NCLE solver have been demonstrated for advanced rotorcraft modeling and simulation:

- Solving the governing equations in fixed or rotating reference frames simultaneously.
- Rotor blades can be treated as actuator disk or actual rotating blades.
- Realistic blade motion including cyclic blade-pitch motion.
- Loosely coupling with elastic blade deformation.
- Realistic rotating-blade/fuselage clearances (2% and 3.4% of rotor disk diameter were demonstrated).
- 6-DOF maneuvering simulation for tiltrotor aircraft with rotating blades.
- Complete rotorcraft simulation in hover, forward flight, and various descent flight conditions.
- Coupling for two-dimensional airfoils with an icing model capable of treating complex porous ice structures.
- Solving both low- and high-speed viscous flows with an arbitrary Mach number solution algorithm.
- Viscous sublayer resolution such that y+ < 1 at all surface points.
- Large time steps corresponding to 1~1.5 degrees of blade rotation per step, selection based on physics and accuracy considerations rather than numerical stability restrictions.
- Efficient runtimes and parallel efficiency for multiple parallel platforms (Sun E10000, SGI R12000, Cray T3E, Linux Cluster).

2.3 Visualization and Animation Software

The visualization and especially the animation of complete rotorcraft simulations has presented a significant challenge due to the very large datasets produced by time-accurate three-dimensional viscous flow simulations with rotating blades, using grids of between five to ten million points. Datasets of order 100 GB are typical, and visualization capabilities have been developed to enable such animations in the SimCenter's DIVA visualization software [11] to allow processing of these very large data sets efficiently. All viewgraphs for the NACA0015 wing solutions reported here were produced by the flow visualization software DIVA, and animations of the three-bladed rotor flow simulations (see Sec. 4) that include high frequency blade-pitch oscillation have also been produced with DIVA. The following Figure 2 shows the iso-swirl parameter over the NACA0015 wing visualized by DIVA, indicating the strength of tip vortex generated in the flow field. These computed and animation results graphically demonstrate that the unsteady flow behavior associated with the wing and rotor can be simulated.

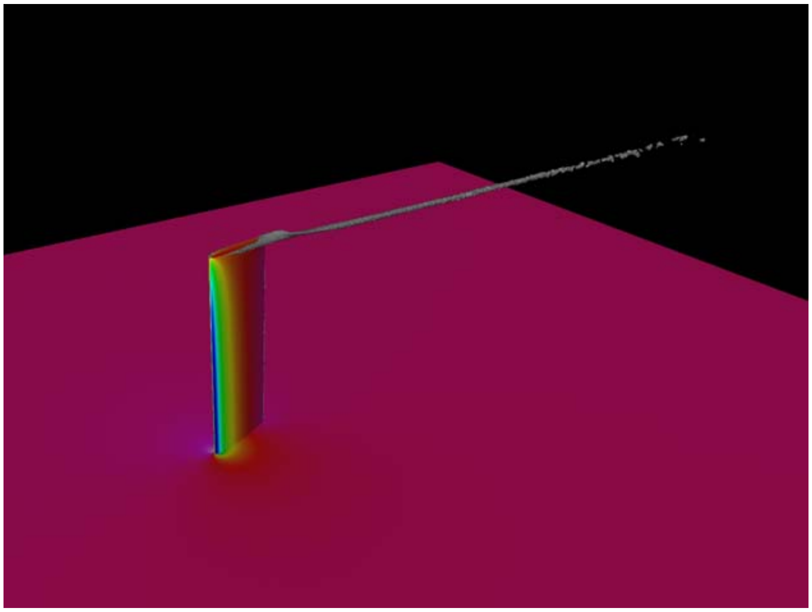

Figure 2 – Iso-swirl parameter and wing surface pressure visualized by SimCenter's visualization software DIVA

2.4 User Community

SimCenter's unstructured simulation system has been distributed to several governmental agencies and industries for computational simulation and design analysis. Major users of the unstructured grid generation include: Boeing, Rocketdyne, Lockheed-Martin, DIA-MSIC, NASA-Marshall, PET program, in addition to many DoD centers that use the software, such as NSWC-Carderock, NSWC-Patuxent River, etc.

The U^2NCLE solver has been transferred/distributed to NSWC-Carderock, DIA-MISC, and ARL/VTD. The U^2NCLE solver is currently being used to conduct CFD analysis of QUAD aero interactions for Bell Helicopter Textron, Inc. in support of Army's Joint Heavy Lift Rotorcraft efforts. The U^2NCLE simulation package will be transferred to Bell Helicopter under a contract agreement by the end of this year.

In additional to the software transfer, techniques and algorithms developed at the SimCenter/MSU have been transferred to the Air Force Research Laboratory/Air vehicles Directorate to enhance the low Mach number capability for the Air Vehicles Unstructured Solver (AVUS).

The following is a list of key users of the U^2NCLE solver:

- Dr. Joe Gorski
  Naval Surface Warfare Center-Carderock Division, MD
  Phone: 301-227-1930, Email: gorskijj@nswccd.navy.mil
- Dr. Alan Nicholson
  Missile and Space Intelligence Center, Huntsville, AL
  Phone: 256-313-7418, Email: lan@msic.dia.mil
- Dr. Michael Hathaway
  U.S. Army Research Laboratory/Vehicle Technology Directorate
  Phone: 216-433-6250, Email: Michael.D.Hathaway@grc.nasa.gov
- Jim Narramore
  Bell Helicopter Textron, Inc., Fort Worth, TX
  Phone: 817-280-5067, Email: jnarramore@bellhelicopter.textron.com

3. Computed Results

3.1 Grid Resolution Study

A series of mixed-element unstructured meshes with various surface resolutions has been generated with the unstructured grid generation system SolidMesh and AFLR. Grid refinement study has been conducted for the NACA0015 wing at 12 degrees angle of attack using U^2NCLE unstructured flow solver. Computed forces and moment over three NACA0012 meshes are given in Table 1, which shows only slight differences in calculated integrated surface loads among these meshes. Therefore, only solutions obtained from the second grid (3.66M node points) were reported here.

Computed lift, drag, and pitching moment coefficients reported here are defined as:

$$C_l = Lift / A_p q_\infty \,; \quad C_d = Drag / A_p q_\infty \,; \quad C_m = Moment / cA_p q_\infty$$

where $q_\infty = \frac{1}{2}\rho v_\infty^2$ is the dynamic pressure, and A_p is the wing planform area estimated as $A_p = c \times s$, c is the airfoil chord, and s is the airfoil half-span since only half a wing physically mounted on the wall for the test problem.

Grids and Turbulence Models		C_l=Lift/(A_p*q_∞)	C_d=Drag/(A_p*q_∞)	C_m=Moment/(c*A_p*q_∞)
Grid 1 1.57M	SA	-	-	-
	kω	0.886	0.063	0.012
Grid 2 3.66M	SA	0.901	0.061	0.010
	kω	0.891	0.063	0.011
Grid 3 7.00M	SA	0.878	0.064	0.0094
	kω	-	-	-

Table 1 – Computed integrated surface loads over three unstructured meshes

3.2 Steady State Simulations

Steady state simulations for the NACA0015 wing were carried out in parallel using 64 processors on a Linux cluster. The wing was positioned at 12 degrees angle of attack, with a free stream (reference) Mach number of 0.1235 and a Reynolds number of 1.5 million based on the airfoil chord length. One-equation Spalart-Allmaras and two-equation κ–ω turbulence models have been used in the current simulations. For a steady state solution, a local time steeping is used, with a maximum CFL number of 40 for Spalart-Allmaras model and 10 for κ–ω turbulence model. Since the steady state simulation does not require temporal accuracy, only one Newton iteration is used at each time step, with 10 symmetric Gauss-Seidel relaxations at each Newton step. The current U^2NCLE solver has a low Mach number capability designed for low-speed flow calculations using a preconditioning technique. This capability can be easily turned on or off through a control parameter in the U^2NCLE input file. Numerical tests have been performed for the NACA0015 wing with and without preconditioning, and convergence and accuracy of these solvers have been evaluated. Figure 3 shows the convergence histograms of preconditioned and non-preconditioned solutions with Spalart-Allmaras and κ–ω turbulence models. With the preconditioning, solutions of both turbulence models show further reduction in residual comparing to the non-preconditioned counterparts.

Computed lift, drag, and pitching moment coefficients are shown in Figures 4-6. Computed forces/moment by the preconditioned scheme reached to a steady state much quickly than the ones without using the preconditioning, indicating a significant savings in computing time for low Mach number flows. Furthermore, differences in integrated surface loads on the wing were observed between preconditioned and non-preconditioned solutions, due to the difference in numerical flux formulations between the two schemes. Generally speaking, a preconditioned solution offers a better accuracy and convergence than a non-preconditioned solution at low Mach numbers.

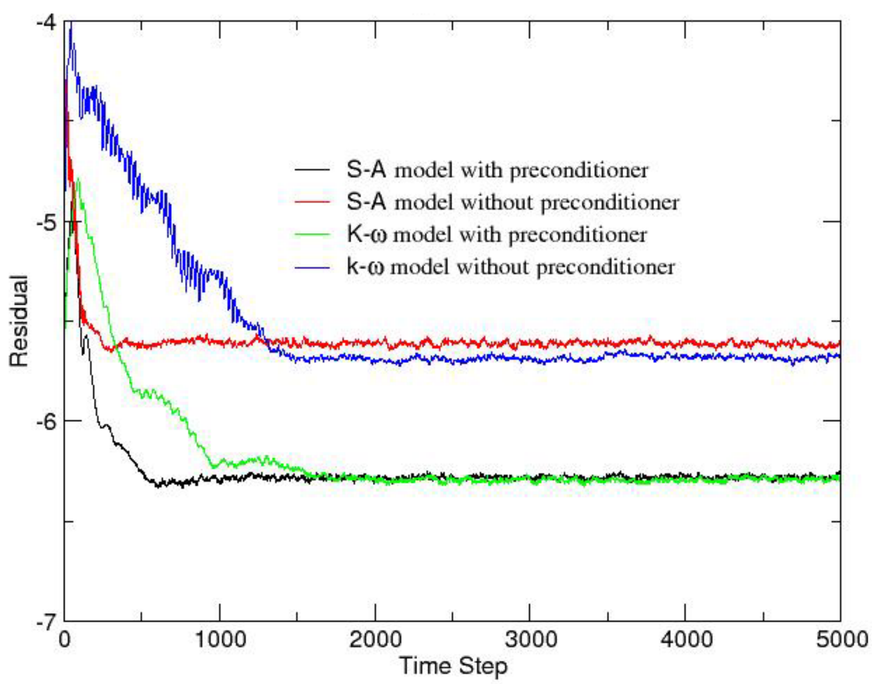

Figure 3 – Convergence histories with and without preconditioning

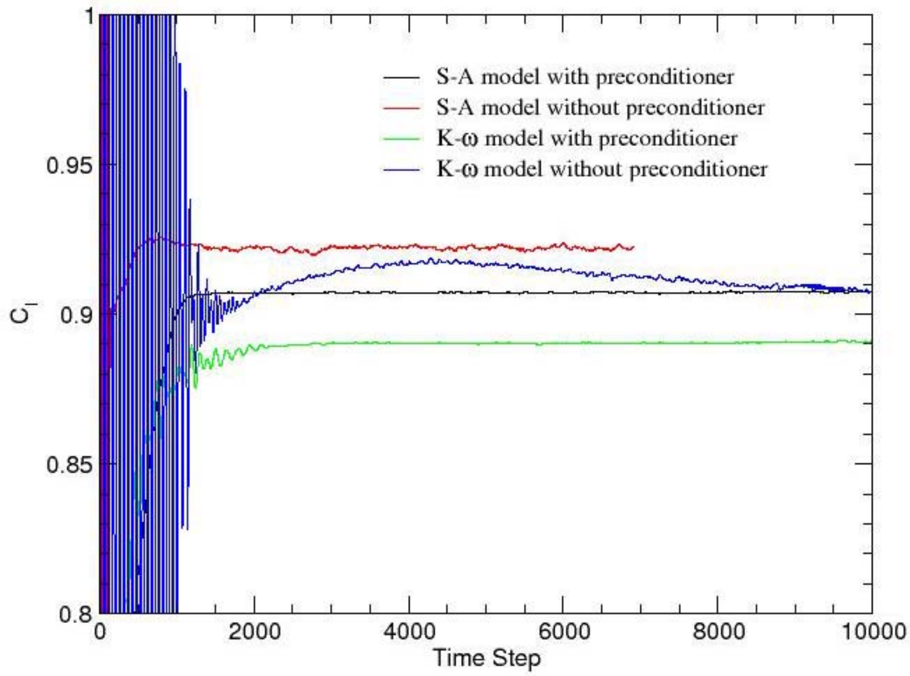

Figure 4 – Computed lift coefficients with and without preconditioning

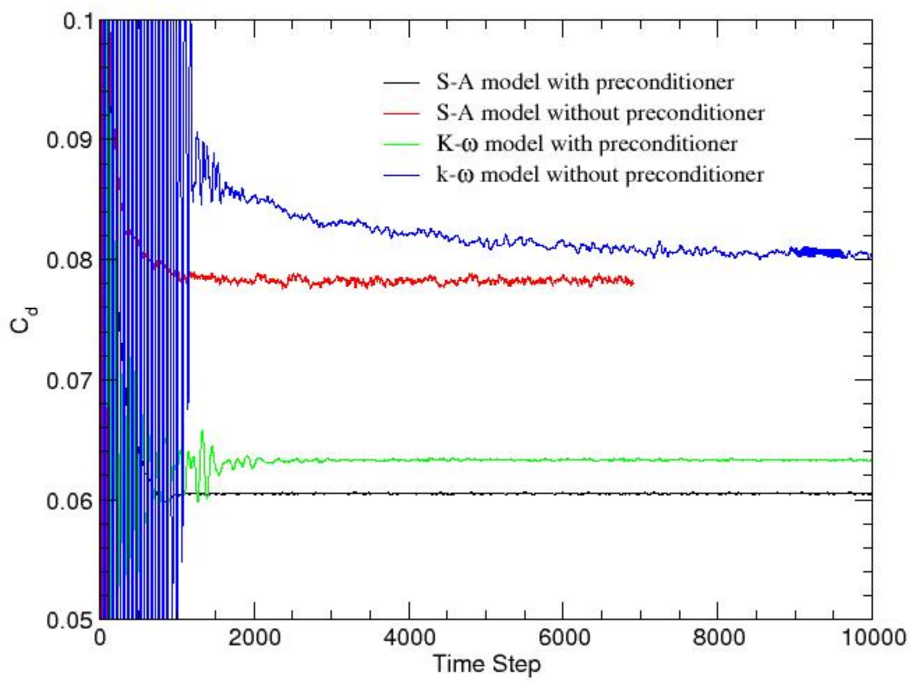

Figure 5 – Computed drag coefficients with and without preconditioning

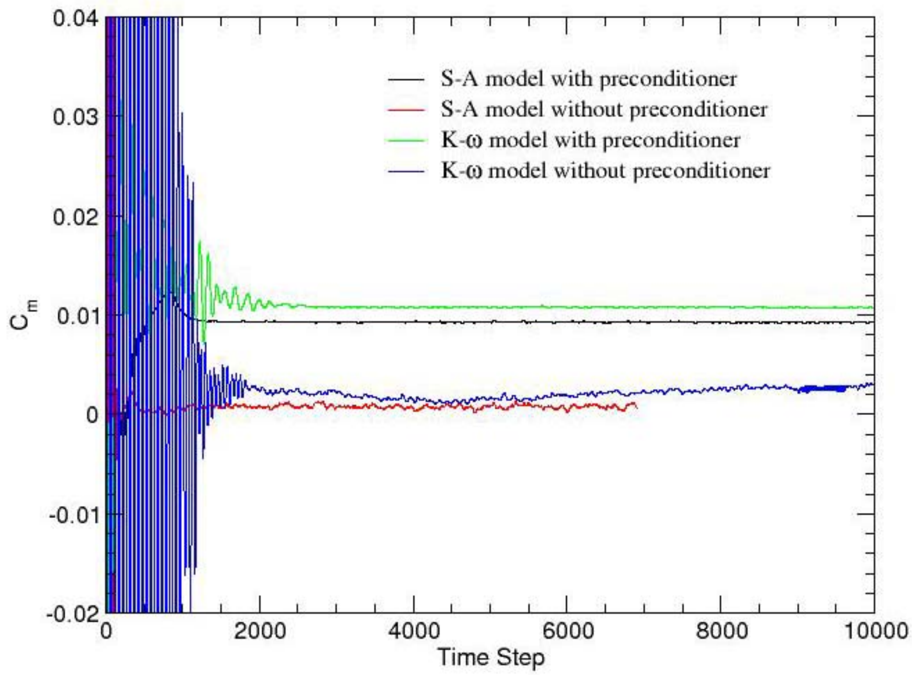

Figure 6 – Computed moment coefficients with and without preconditioning

3.4 Time-Accurate Simulations

The unsteady time-accurate simulations were performed with a second-order temporal accuracy using a minimum time step of 0.002, which is equivalent to 500 time steps per characteristic time. The characteristic time T is the non-dimensional time required for a particle moving at the free stream velocity to travel one chord length. Simulations were carried out on a Linux cluster using 64 processors. The numerical tests have been conducted to evaluate the effect of multiple Newton iterations for unsteady runs. Figure 7 shows convergence histories of time-accurate simulations using 1, 2, and 4 Newton iterations. The results show that multiple Newton iterations at each time step significantly speed up the solution process to the final state for the test problem. However, the cost of CPU time is also increased accordingly. Time histories of integrated lift, drag, and pitch moment coefficients on the wing are plotted in Figures 8-10, where a $\kappa-\omega$ turbulence model was used. By comparing the relative errors of computed unsteady surface loads at a characteristic time of 15T with the final converged (steady state) solutions, it seems that the time-accurate solution with 2 Newton iterations per time step is the most cost-effective way to reach a steady state for the current test problem. However, it is recommended that 3 to 4 Newton iterations be used at each time step to achieve the temporal accuracy for complex unsteady simulations. Figures 11-20 show Cp distributions at different wing span locations obtained with 4 Newton iterations at a characteristic time of 15T. Computed results from the converged steady state solution were also shown in the figures for comparison purpose. A preconditioning scheme is used for all of the time-accurate unsteady solutions shown here.

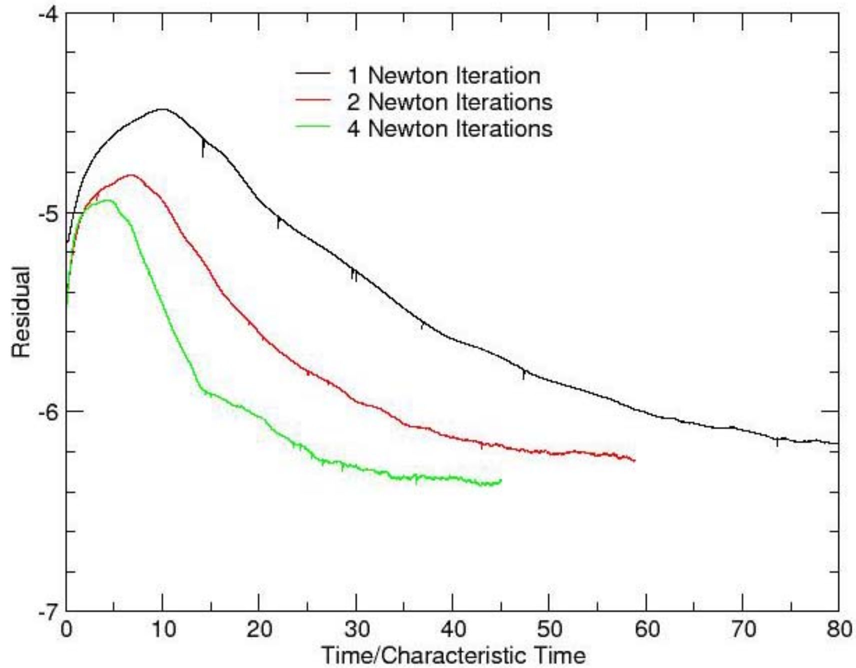

Figure 7 – Convergence of time-accurate solutions with multiple Newton iterations and κ−ω turbulence model

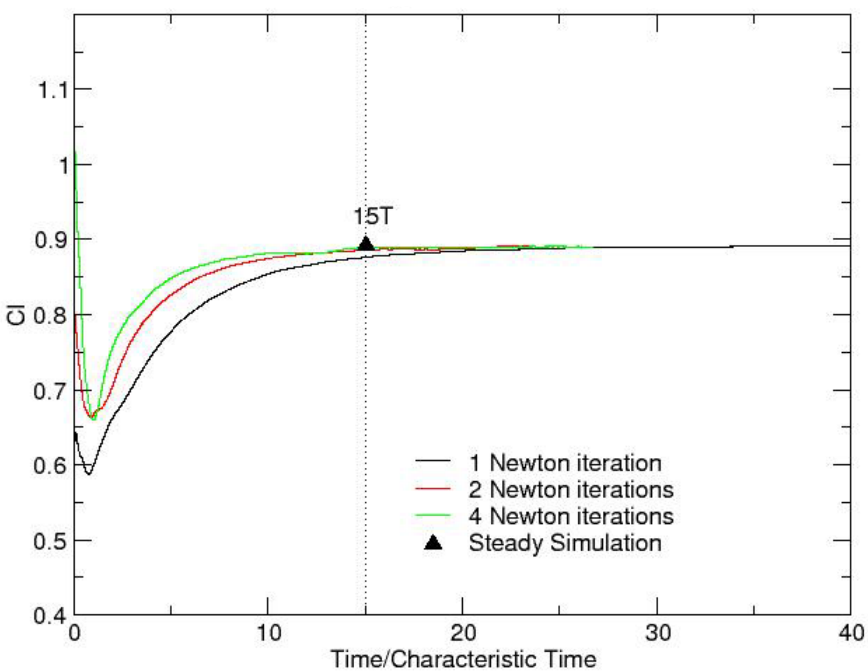

Figure 8 –Time history of integrated lift coefficients

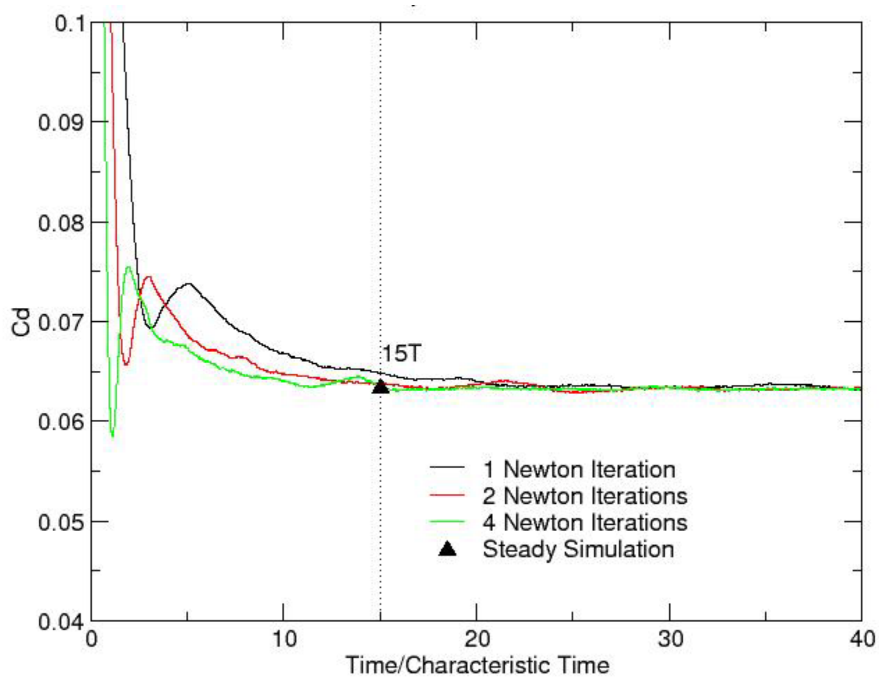

Figure 9 – Time history of integrated drag coefficients

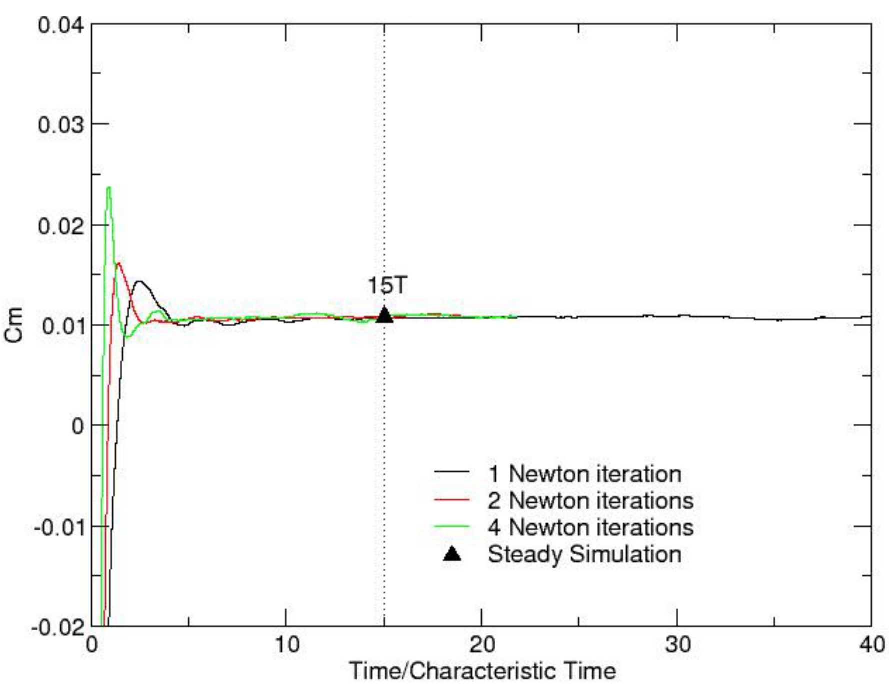

Figure 10 – Time history of integrated pitching moment coefficients

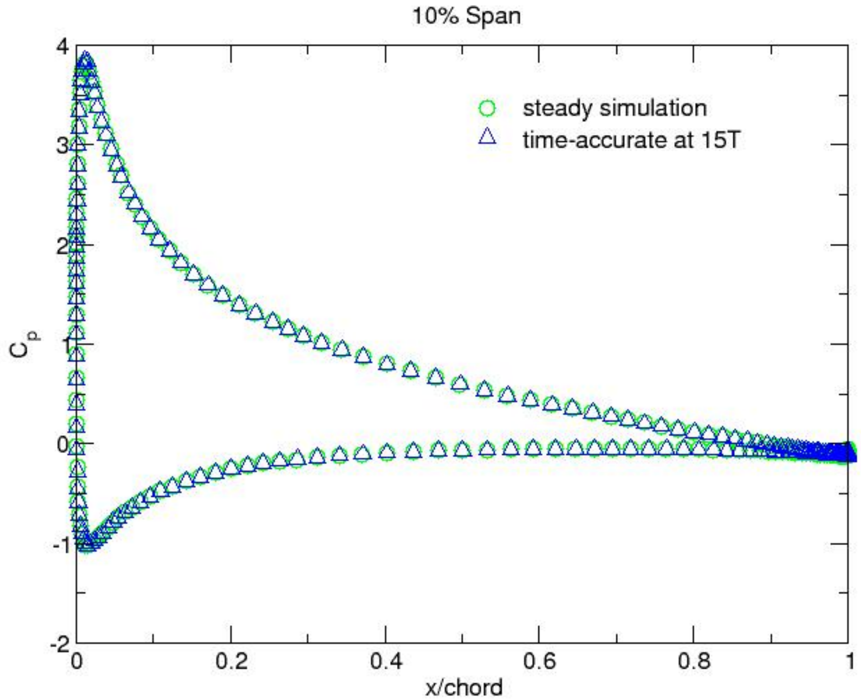

Figure 11 – Computed Cp distributions at 10% span

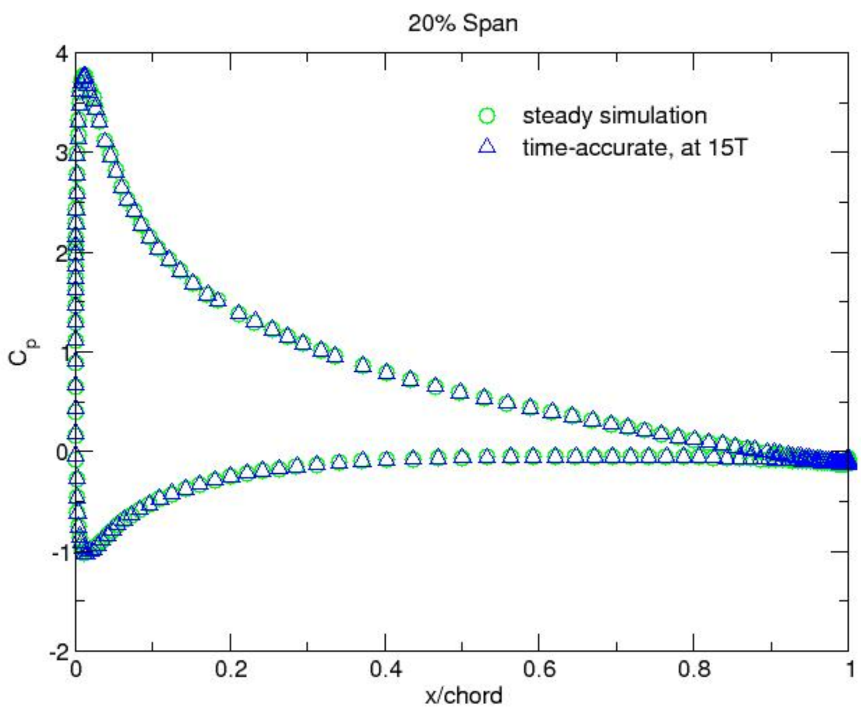

Figure 12 – Computed Cp distributions at 20% span

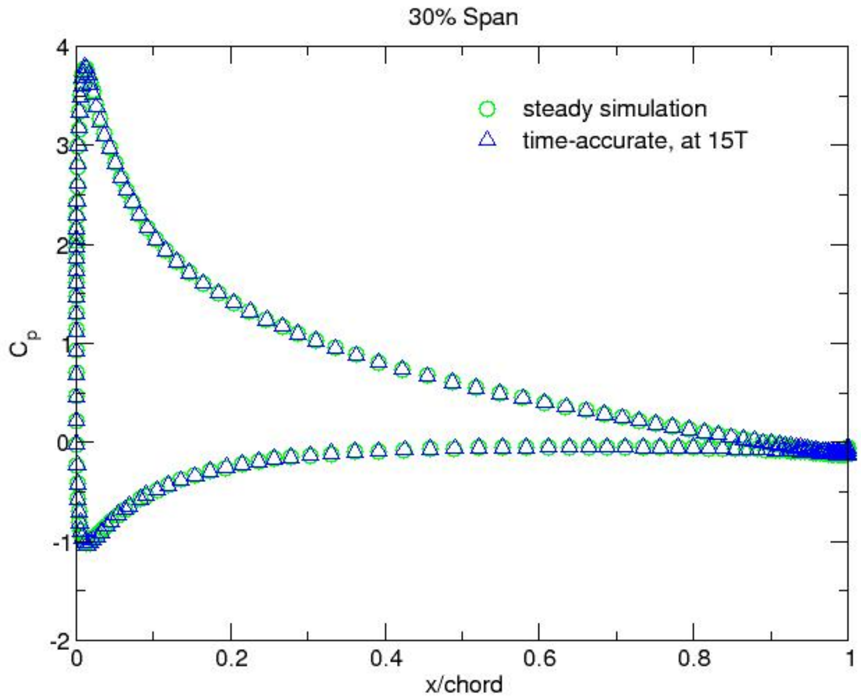

Figure 13 –Computed Cp distributions at 30% span

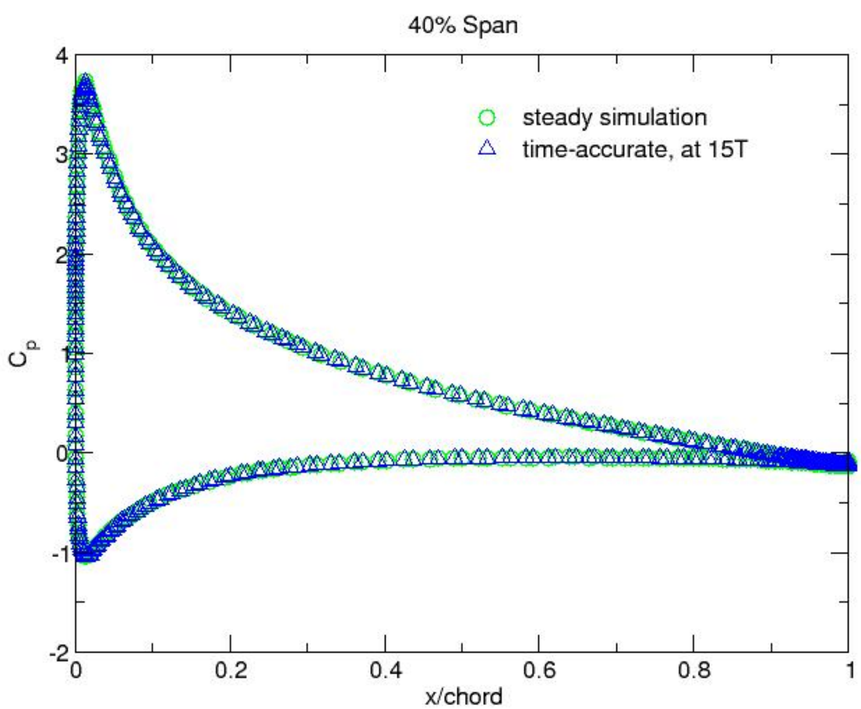

Figure 14 – Computed Cp distributions at 40% span

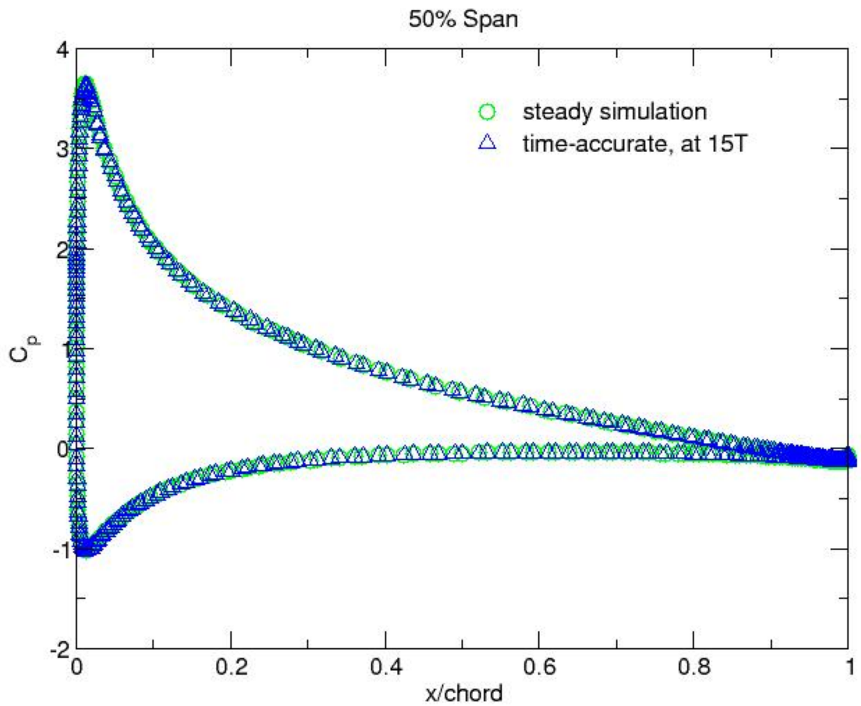

Figure 15 – Computed Cp distributions at 50% span

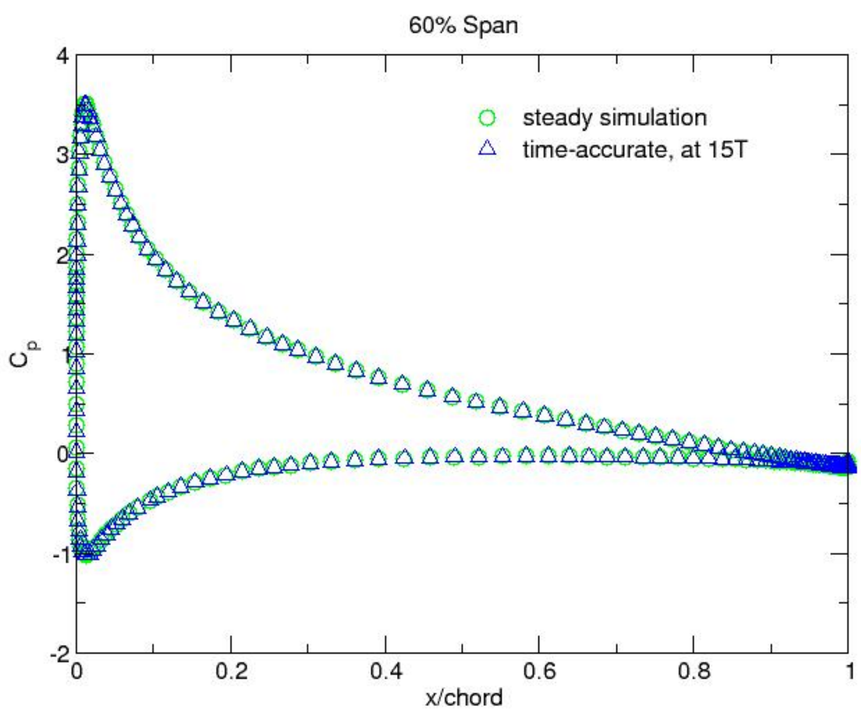

Figure 16 – Computed Cp distributions at 60% span

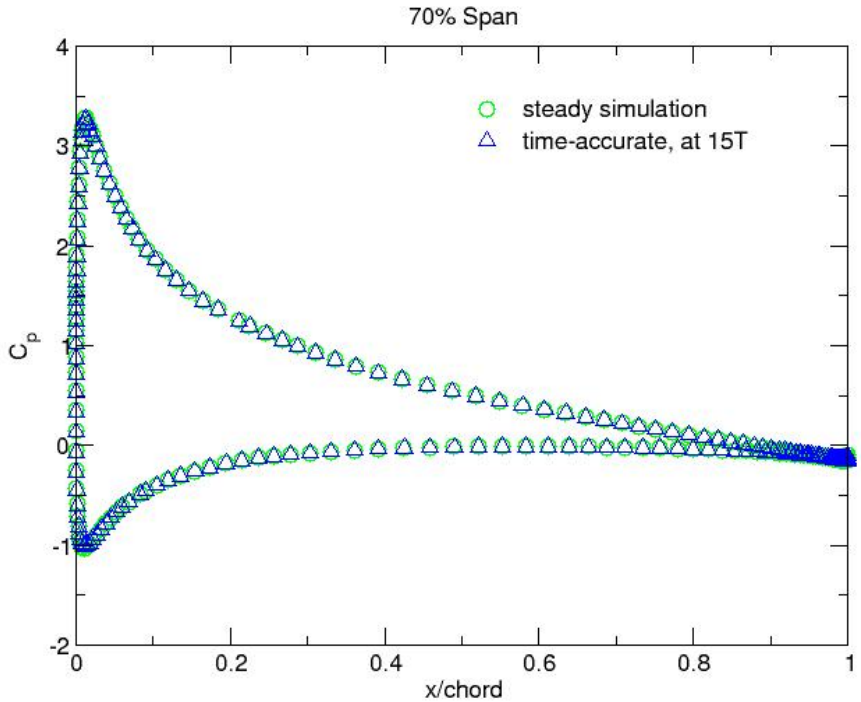

Figure 17– Computed Cp distributions at 70% span

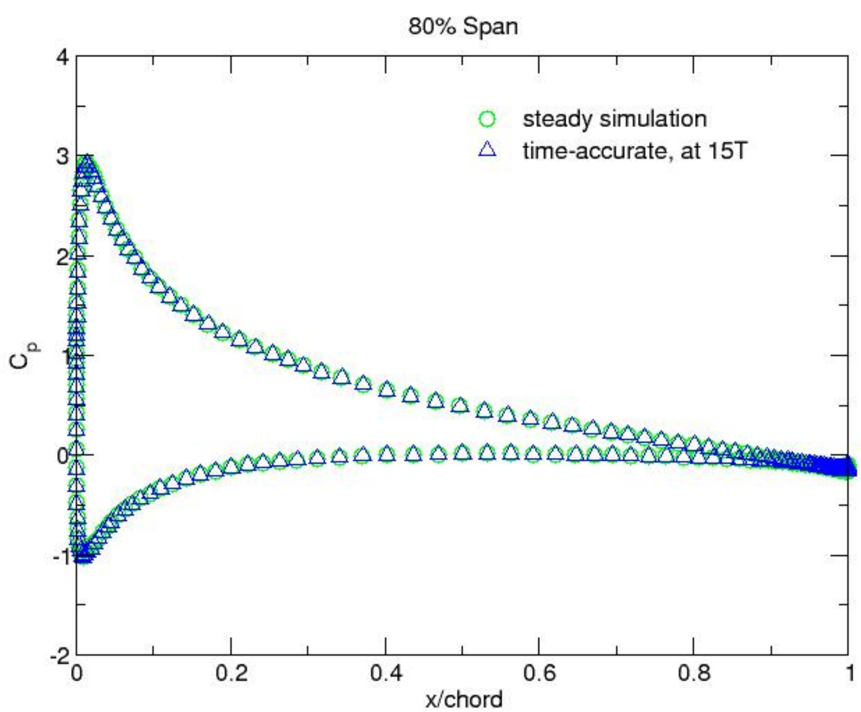

Figure 18 – Computed Cp distributions at 80% span

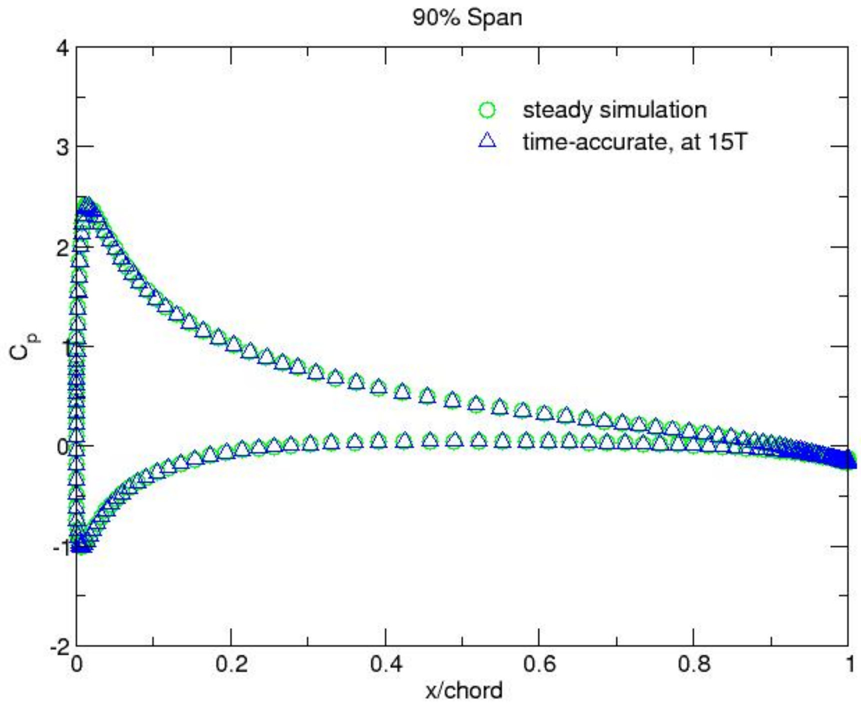

Figure 19 – Computed Cp distributions at 90% span

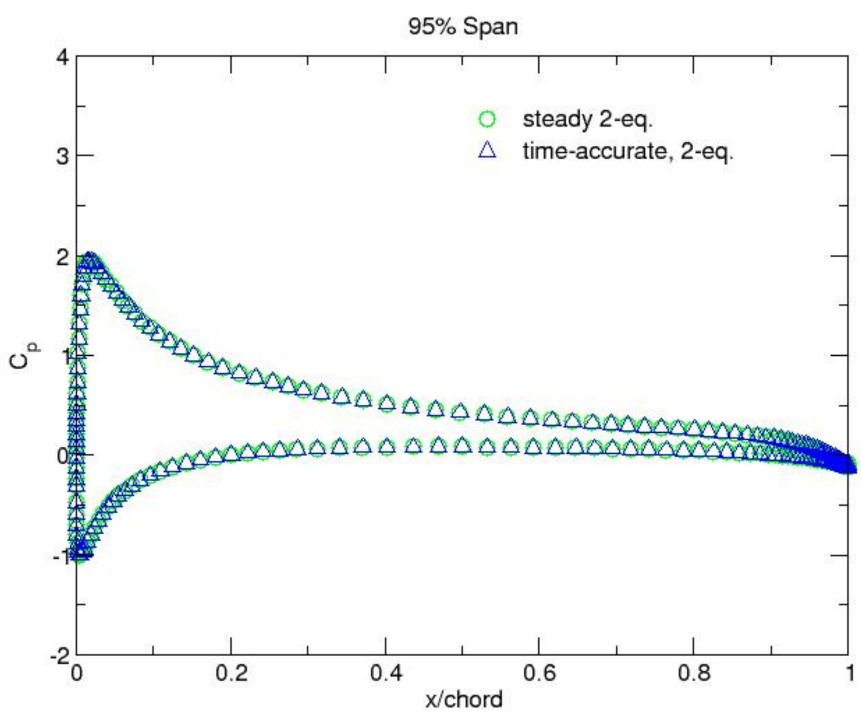

Figure 20 – Computed Cp distributions at 95% span

3.5 Performance and Statistics

The scalability of this flow solver for a Linux supercluster with 32, 64, 128, and 256 processors is shown in Figure 21 for the test problem with 3.66M points. Memory and CPU time usages are listed in Table 2. The unstructured solver is MPI portable across a wide of computer platforms, and the present results have been obtained on a 874-processor Linux Supercluster (IBM x330 1.266 GHz Pentium III, 1.3 GB RAM per node).

For the steady simulation using 64 processors, the total CPU time required for a converged solution using a Spalart-Allmras model is 357 hours (sum of CPU time on 64 processors for 600 time steps). For the unsteady time-accurate simulation using 4 Newton iterations and $\kappa-\omega$ turbulence model, the total CPU time required to run 15T is 4467 hours (sum of CPU time on 64 processors for 7500 time steps). All CPU times were counted based on the Linux cluster mentioned above.

The parallel algorithms for unstructured and structured grids are closely related and have similar scalability properties. The scalability properties of the structured-grid algorithm have been studied for generic architectures in [6]. A semi-empirical performance model was developed to study the scalability of the parallel solution algorithms as actually implemented for existing and 9 hypothetical computing platforms using MPI message passing. The model defines and estimates three parallel efficiencies (CPU, cost and memory efficiencies), and results are shown in Figure 22 for a generic computer having the following parameters: effective CPU (100Mflops) and buffering (30Mb/s) rates, MPI bandwidth (130Mb/s) and latency (15ms), and memory of 512Mb per processor. These are shown for both memory-constrained size-up in which the problem size is increased to maintain 100% memory utilization as processors are added, and a constant-problem-size scale-up for 10 million grid points. As expected, the CPU efficiency is higher for memory-constrained size-up, but the difference in cost efficiency is more dramatic due to the rapid drop in memory efficiency for constant problem size.

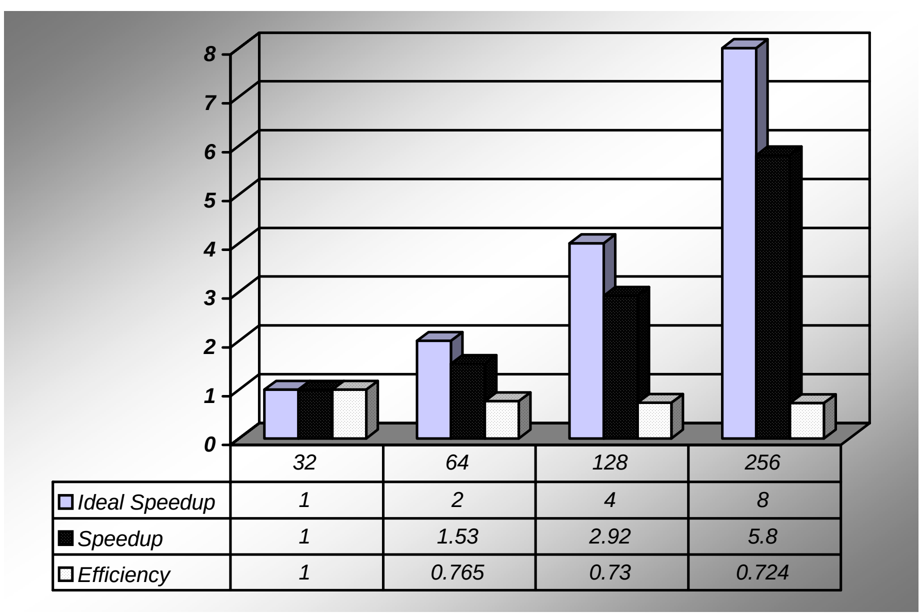

Figure 21 – Relative efficiency and speedup of U²NCLE solver on a Linux cluster for the test problem with 3.66M node points

Number of Processor	Memory per processor (MB)	CPU Time per Step (Seconds)	Total CPU Time* (Hours)
32(N)	549	175.5	4.87
64(2N)	287	114.6	3.18
128(4N)	145	60.4	1.67
256(8N)	85	30.3	0.84

Table 2 – Memory and CPU time usages per processor on a Linux cluster for the test problem with 3.66M node points

*Total CPU time per processor required to run 100 steps in time-accurate mode
4 Newton iterations used at each time step

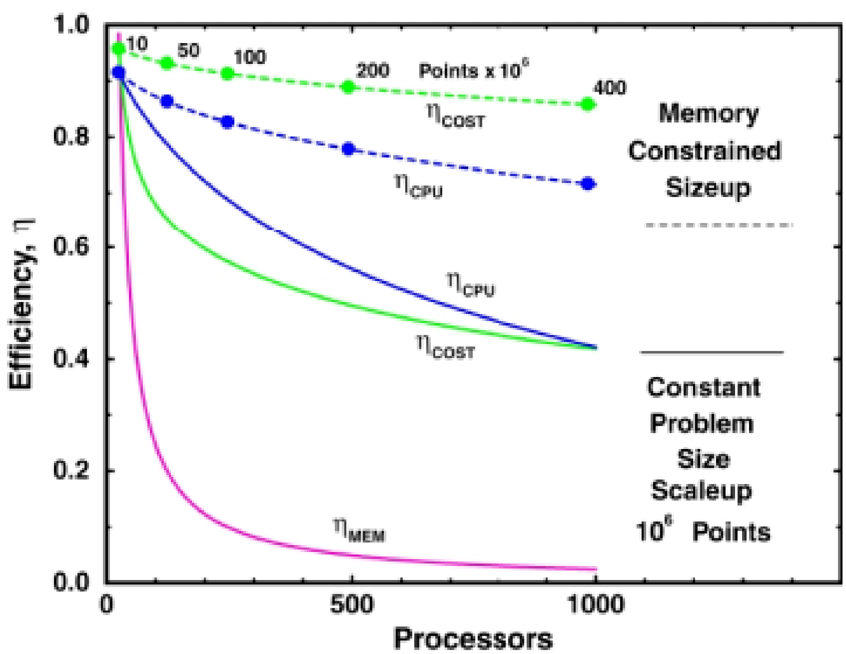

Figure 22 – Scalability properties from a semi-empirical performance model

The most important computer parameters for scalability are effective CPU rate as timed for the executable operating with message passing suppressed, the MPI software bandwidth for large messages, and the time required to load message-passing buffer arrays. The MPI latency is negligible since there are only a small number of large messages. Overall, the performance model indicates that the method is scalable in a practical sense for large-scale problems.

4. Optional Results

4.1 Overview

The optional test problem considered in the current grant is a realistic three-bladed rotor. It has a radius of 13 ft. The tip speed is 775.0 ft/s and the tip Mach number is 0.69. The Reynolds number is 99 million based on the diameter of the blade and the tip velocity. The reason of choosing this configuration is to demonstrate the unique capability of the U^2NCLE solver to simulate realistic rotor blade motion including cyclic pitching. A high-frequency blade-pitch oscillation is introduced to the hovering and descending rotor. Each blade is oscillating around its own axis at a pitch rate of 4 cycles per rotor revolution and at an amplitude of 5 degrees. This simulation intends to mimic a Higher Harmonic Control (HHC) experiment conducted at NASA Ames Research Center for reducing blade-vortex interaction (BVI) noise for XV-15 Rotor [12].

4.2 Unstructured Grid

The computational mesh for the isolated rotor was generated with the SimCenter's unstructured grid generation tools SolidMesh and AFLR. The mesh has 2.29 million nodes and 7.97 million mixed elements. The mesh points are packed near the solid surface, resulting in boundary layer mesh with y^+ value of about one off the solid surface. An overall view of the isolated rotor mesh and a close view of the boundary layer mesh near the blade tip are shown in Figure 23.

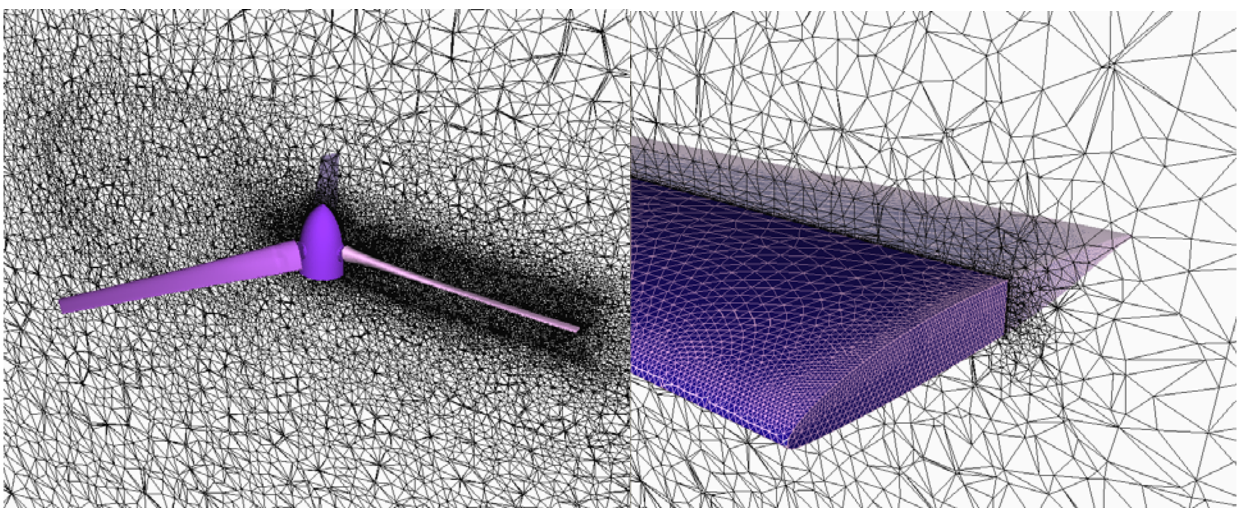

Figure 23 – An overview and a close-up view of the unstructured mesh for the optional test problem

4.3 Rotor in Hover

First, the rotor in hover is modeled with the U^2NCLE solver. A high-frequency blade-pitch oscillation is imposed on each individual blade for cyclic motion. The instantaneous blade pitch angle is given by $\alpha(t) = \alpha_0 + \alpha_1 \sin(\omega t)$, where α_0 is the collective angle and α_1 is the alternating pitch angle (amplitude of the oscillation). In the current configuration, the collective angle is preset and alternating pitch angle is chosen at 5 degrees. The input pitch rate is 4 cycles per blade revolution. A time-accurate viscous flow simulation was performed using 4 Newton iterations and 10 Gauss-Seidel relaxations at each time step, which is required to maintain the temporal accuracy and stability for the current simulation. The minimum time step used is 0.000292954 seconds throughout the simulation, which corresponds to one degree of the rotor rotation per time step. A periodical solution is established around 2000 time steps, or about 5 rotor revolutions. This is equivalent to 28 hours of CPU time based on the Linux cluster mentioned before.

A strong tip-vortex generated by the rotor blade is the main feature of the unsteady flow field, where the trajectory of the tip-vortex can last several revolutions in the downwash flow. Figures 24 and 25 show the instantaneous swirl parameter and Mach number on the rotor disk cutting plane. Unsteady vortex patterns of the tip-vortex flow are observed at different phases during the blade upstroke and downstroke oscillating cycle. The complex flow behavior associated with the blade pitch oscillation is clearly demonstrated by the current unstructured solver.

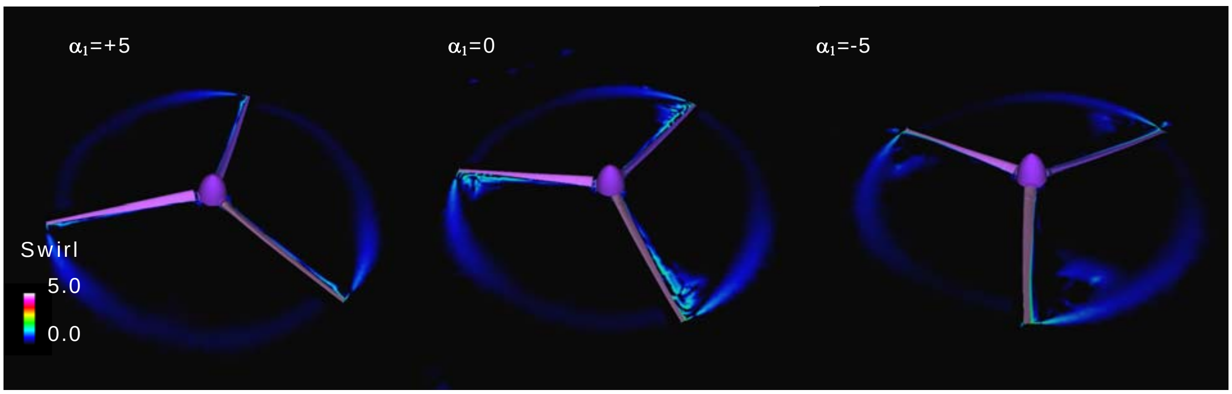

Figure 24 - Computed swirl parameter on rotor disk cutting plane during downstroke of blade oscillating cycle

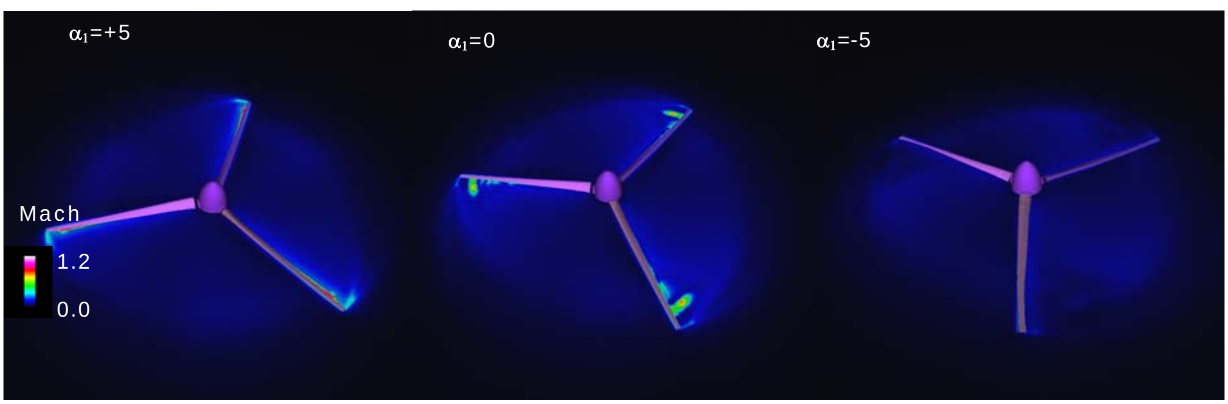

Figure 25 - Computed Mach number on rotor disk cutting plane during downstroke of blade oscillating cycle

4.4 Rotor in Decent

The rotor in descent condition is also simulated and presented. The purpose here is to simulate and demonstrate the complex three-dimensional unsteady blade-vortex interaction (BVI) in a forward and descent (approaching) condition, and reveal the effect of active blade-pitch control to the flow field. The simulation was performed in a similar manner as the previous simulation, except that the free stream flow has an advance ratio (ratio of the forward speed to blade tip speed) is 0.15, and rotor descent angle is 8 degrees. The blade pitch rate and angle remain the same as the previous case. The flow condition is considered a low speed forward-descent flight, where the blade-vortex interaction is dominated in the flow field.

For rotor without blade-pitch oscillation, a strong tip vortex induced by the advancing blade is clearly seen in the flow field, as shown in Figure 26 by the swirl parameter on the rotor-disk cutting plane. With the blade-pitch oscillation, the trajectory of the tip vortex generated by the advancing blade is significantly different from that without blade-pitch oscillation, as shown in Figure 27. This certainly affects the way how the blade interacts with the vortex, and thus the BVI noise. The computational capability demonstrated in the current unstructured solver may provide better understanding to this complex flow phenomenon and underlying mechanism to the BVI noise reduction by active blade-pitch control.

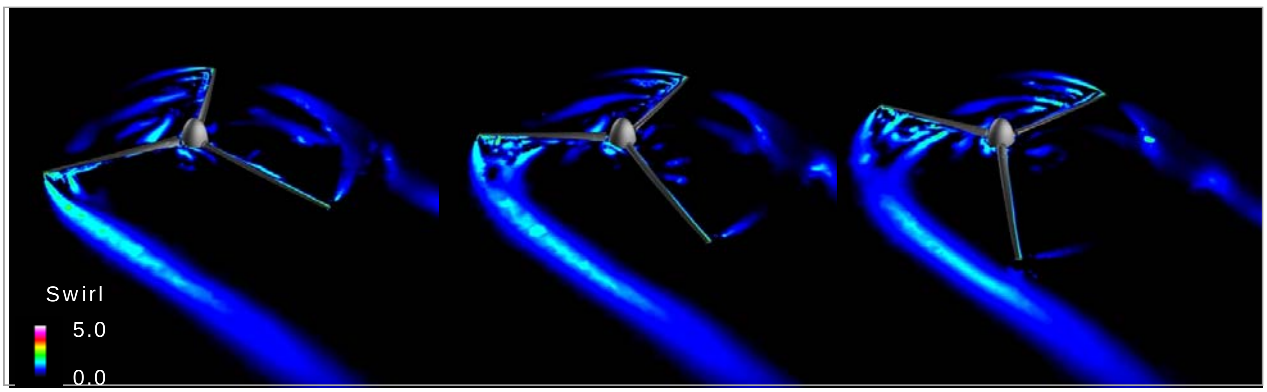

Figure 26- Computed swirl parameter on rotor disk plane without blade oscillation

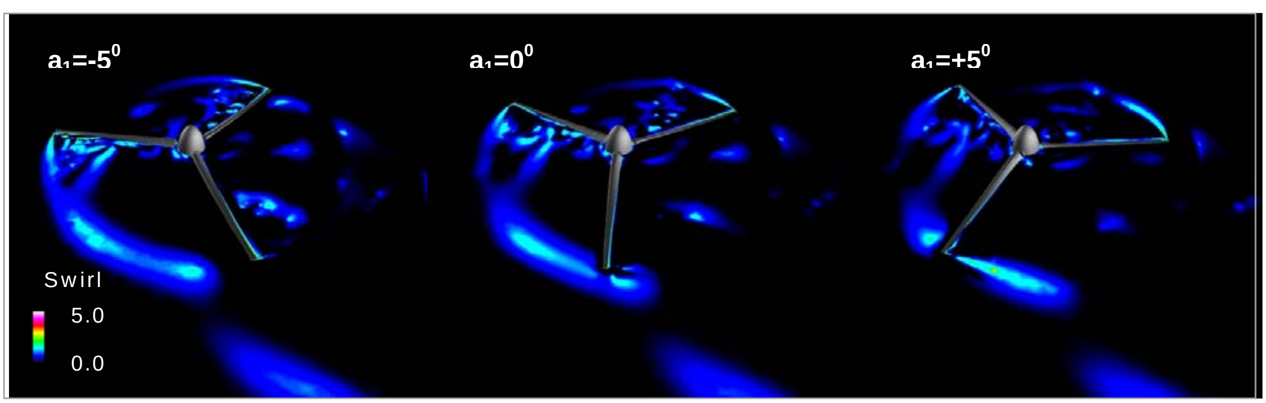

Figure 27 - Computed swirl parameter on rotor disk plane with blade oscillation

5. Technology Transfer

5.1 Solution Transfer

Unstructured grid and solutions produced for the common test problem NACA0015 wing have been transferred to Dr. Robert Meakin at Army Aeroflightdynamics Directorate at NASA Ames Research Center. This includes an unstructured volume grid with 3.66M node points, a time-accurate solution and surface Cp distributions at a specified characteristic time 15T obtained by the U^2NCLE solver with κ-ω turbulence mode, the convergence history of the forces/moment, the solver input and boundary condition files to run the unstructured solver U^2NCLE.

5.2 Software Transfer

Unstructured simulation package was successfully transferred to Dr. Robert Meakin at Army Aeroflightdynamics Directorate at NASA Ames Research Center in April 2006. Three versions of the source code (incompressible, compressible, and arbitrary Mach number) for U^2NCLE were released. To supplement the source code, an instruction note and a web-based tutorial describing the general features of U^2NCLE were delivered in the package to Dr. Bob Meakin (AFDD). A password-protected ftp site at SimCenter/MSU has been set up for downloading the following simulation packages upon request:

- SolidMesh (SimCenter's surface grid generator)
- AFLR (SimCenter's volume grid generator)
- DIVA (SimCenter's visualization/animation software)
- U^2NCLE (SimCenter's unstructured flow solver, including incompressible, compressible, and arbitrary Mach number versions)
- USS_U^2NCLE (SimCenter's user interface software for grid generation, flow solver, and visualization)
- Miscellaneous Unstructured Grid Tools (checkgrid, extract, gc, gridmerge, part, pcut, ptrace, relframe, scalegrid, scaleflow, slice, surftool, ugc, ugio2cgns, ugio2u2ncle, unpart, unpartsurf, voltool, vortex)

6. Summary

Steady and unsteady time-accurate simulations have been performed with the SimCenter's unstructured solver U^2NCLE for the common test problem, the NACA0015 wing. Results and computational statistics from these simulations have been obtained and presented in the current report. In addition, unsteady time-accurate simulations have been performed on an optional test problem about a generic but realistic three-bladed rotor undergoing high frequency blade-pitch motion. Among many useful features in the U^2NCLE simulation system, the following remarks are worth to mention which might be of interest to the HI-ARMS evaluation team:

- Performance and computational statistics indicate that the U^2NCLE solver is scalable in a practical sense for large-scale problems.

- The arbitrary Mach number version of the U^{2}NCLE solver allows calculation of both low- and high-speed viscous flows, with demonstrated benefit in convergence/accuracy in predicting low Mach number flows.
- Dynamic motion grid capability in the U^{2}NCLE solver allows simulation of complete rotorcraft with actual rotating blades undergoing cyclic blade motion in a fully conservative way.

References

1. Marcum, D.L., ”Unstructured Grid Generation Using Automatic Point Insertion and Local Reconnection,” The Handbook of Grid Generation, edited by J.F. Thompson, B. Soni, and N.P. Weatherill, CRC Press, p. 18-1, 1998.
2. Marcum, D.L. and Gaither, J.A., “Unstructured Surface Grid Generation Using Global Mapping and Physical Space Approximation,” 8th International Meshing Roundtable, South Lake Tahoe, CA, October 1999.
3. Marcum, D.L. and Gaither, J.A., “Mixed Element Type Unstructured Grid Generation for Viscous Flow Applications,” AIAA-99-3252, 14th AIAA Computational Fluid Dynamics Conference, Norfolk, VA, June 1999.
4. Hyams, D.G., Sreenivas, K., Sheng, C., Briley, W.R., Marcum, D.L., and Whitfield, D.L., ”An Investigation of Parallel Implicit Solution Algorithms for Incompressible Flows on Multielement Unstructured Topologies,” 38th Aerospace Sciences Meeting & Exhibit, AIAA Paper No. 2000-0271, Reno, NV, January 2000.
5. Hyams, D.G., “An Investigation of Parallel Implicit Solution Algorithms for Incompressible Flows on Unstructured Topologies,” PhD Dissertation, Mississippi State University, May 2000.
6. Pankajakshan, R., Taylor, L. K., Sheng, C., Briley, W. R., and D. L. Whitfield, “Scalable Parallel Implicit Multigrid Solution of Unsteady Incompressible Flows”. Frontiers of Computational Fluid Dynamics 2000, Edited by D. A. Caughey and M. M. Hafez, World Scientific Publishing Company PTE. LTD., Singapore, 2001, pp. 181-195.
7. Briley, W.R., Tayler, L.K., and Whitfield, D.L.,“High–Resolution Viscous Flow Simulations at Arbitrary Mach Number,” *Journal of Computational Physics*, 184(1), 79–105, 2003.
8. Sheng, C., Newman III, J., Remotigue, M., Chen, J.P., Marcum, D, and Whitfield, D., “Development of Unstructured Computational Capabilities Applicable to MSU TURBO with an Arbitrary Mach Number Algorithm,” Final Report for NASA Grant NAG 3-1699, MSSU-COE-ERC-02-16, Mississippi State University, October 2002.
9. Sheng, C. and Wang, X., “A Global Preconditioning Method for Low Mach Number Viscous Flows in Rotating machinery” Proceedings of ASME Turbo Expo 2006, GT2006-01189, 8-11 May 2006, Barcelona, Spain.
10. Sreenivas, K., Hyams, D. G., Sheng, C., Jayaraman, B., Wang, X., Mitchell, B., Jiang, M. Y., Pankajakshan, R., Taylor, L. K., Gaither, K. P., Gaither, A., Beeland, H., Marcum, D. L., Briley, W. R., and D. L. Whitfield: Physics-Based Maneuvering Simulations for Tiltrotor Aircraft. MSU Report No. MSSU-COE-ERC-02-06 (NASA-ARC Grant NAG2-1232), April 2002.
11. DIVA Online Manual, Computational Simulation and Design Center, Mississippi State University.
12. Mark Betzina, Khanh Nguyen, and Wayne Johnson, “Tilt-Rotor Noise Reduction Using Higher Harmonic Control,” presentation note, November 1999.